



Original article

Blockade of STAT3 activation by sorafenib derivatives through enhancing SHP-1 phosphatase activity

Kuen-Feng Chen^{b,c}, Wei-Tien Tai^{c,d}, Cheng-Yi Hsu^a, Jui-Wen Huang^f, Chun-Yu Liu^{a,e}, Pei-Jer Chen^{b,h}, InKi Kim^g, Chung-Wai Shiau^{a,*}^a Institute of Biopharmaceutical Sciences, National Yang-Ming University, No. 155, Sec. 2, Linong Street, Taipei, Taiwan^b Department of Medical Research, National Taiwan University Hospital, Taipei, Taiwan^c National Center of Excellence for Clinical Trial and Research, National Taiwan University Hospital, Taipei, Taiwan^d Graduate Institute of Molecular Medicine, National Taiwan University College of Medicine, Taipei, Taiwan^e Division of Hematology and Oncology, Department of Medicine, Taipei Veterans General Hospital, Taipei, Taiwan^f Biomedical Engineering Research Laboratories, Industrial Technology Research Institute, Hsinchu, Taiwan^g ASAN Institute for Life Science, ASAN Medical Center, Seoul, Republic of Korea^h Graduate Institute of Clinical Medicine, National Taiwan University College of Medicine, Taipei, Taiwan

ARTICLE INFO

Article history:

Received 2 May 2012

Received in revised form

2 July 2012

Accepted 15 July 2012

Available online 23 July 2012

Keywords:

Sorafenib

STAT3

SHP-1

HCC

ABSTRACT

Previously, we demonstrated that the multiple kinase inhibitor sorafenib mediates the repression of phospho-STAT3 in hepatocellular carcinoma cells. In this study, we used this kinase-independent mechanism as a molecular basis to use sorafenib as scaffold to develop a novel class of SHP-1-activating agents. The proof of principle of this premise was provided by SC-1, which on replacement of N-methylpicolinamide by a phenylcyano group showed abolished kinase activity while retaining phospho-STAT3 repressive activity. Structural optimization of SC-1 led to compound **6**, which repressed phospho-STAT3 through SHP-1 activation and inhibited PLC5 cell proliferation at sub-micromolar potency. In light of the pivotal role of phospho-STAT3 in promoting tumorigenesis and drug resistance, this novel SHP-1-activating agent may have therapeutic relevance in cancer therapy.

© 2012 Elsevier Masson SAS. All rights reserved.

1. Introduction

Overexpression of signal transducers and activators of transcription 3 (STAT3) has been linked to tumorigenesis in a variety of human cancers [1–7]. Evidence indicates that STAT3 is directly recruited to ligand-induced cytokine receptors. Phospho-STAT3 then dimerizes in the cytoplasm and translocates to the nucleus, where the dimer binds to specific DNA-response elements and regulates STAT3-targeted gene expression [8,9]. For example, the anti-apoptotic proteins, Bcl-2, cyclin D1, and Mcl-1 are transcribed by the activated STAT3 and preclude cell apoptosis upon the treatment with chemotherapeutic agents. The action of interleukin-6-STAT3 signaling underscores the oncogenic potential of STAT3 induction in many forms of cancer, and inhibition of STAT3 activation by small molecules has been shown to block tumorigenesis and reverse the transformed phenotype of human cancer cells [10–13].

The Src-homology protein tyrosine phosphatase (PTP) SHP-1 is a non-receptor phosphatase that negatively regulates cytokine signaling such as that of IL-3R, the PDGF- and EGF receptors, and other tyrosine kinase receptors [14–16]. It has been shown that SHP-1 dephosphorylates STAT3 by IL-6 signaling the preventing STAT3 activation. Moreover, genetic transfection of SHP-1 in breast cancer cells has been shown to reduce cell proliferation [17]. Conversely, siRNA knockdown of SHP-1 expression in prostate cancer cells resulted in increased cellular proliferation [18]. In light of the function of SHP-1 as a tumor suppressor gene, increasing its activity represents a promising strategy for cancer therapy. Previously, we reported that the multiple kinase inhibitor, sorafenib, activated SHP-1 activity independently of kinase inhibition [12,13]. The dissociation of these two pharmacological activities, i.e., SHP-1 activation versus kinase inhibition, provides a molecular basis for using sorafenib as a scaffold to develop novel agents that can effectively activate SHP-1 expression. Here, structural optimization of compounds led to a novel class of SHP-1-activating agents with sub-micromolar potency.

* Corresponding author. Tel.: +886 2 28267930; fax: +886 2 28250883.

E-mail address: cwshiau@ym.edu.tw (C.-W. Shiau).

2. Chemistry

In our previous report, we demonstrated that the replacement of N-methylpicolinamide by a phenylcyano group in the sorafenib scaffold abolished kinase inhibition activity without compromising SHP-1-activating activity. In this study the resulting kinase-inactive analog SC-1 (Fig. 1A) was used as a lead compound. First, to understand the role of the urea group of SC-1 in SHP-1 activation, different substituents were added to the terminal urea of SC-1 yielding compounds **1–12**. Among them, addition of a methylene next to the urea group resulted in compounds **1–5**. Further, we replaced the urea in SC-1 with sulfonylamide, carbonyl amide and amino groups to obtain compounds **7–11**, and a sorafenib moiety was synthesized by the replacement of the urea group with sulfonylamide, carbonyl amide and amino groups to generate compounds **13–17**. We then used the nitro-, amino-, benzoimidazol-2-one substitutions of SC-1 as platforms to carry out structural optimization, which generated compounds **18–24**. These SC-1 derivatives were synthesized according to the general procedure described in Fig. 1B. All derivatives synthesized were racemic compounds except compound **5**.

3. Results

3.1. Pharmacological exploitation of kinase-independent effect of sorafenib on SHP-1 activation to generate a novel class of SHP-1-enhancer agents

The dose-dependent effect of SC-1 on SHP-1 activation in PLC5 cells was examined using an IP-SHP-1 phosphatase activity kit after drug treatment for 24 h (Fig. 2). SC-1, though devoid of kinase inhibition activity, exhibited potent activation of SHP-1. For

example, the concentration required for significant enhancement of SHP-1 activation was approximately the same for SC-1 as for sorafenib. In a previous report, we demonstrated that sorafenib-mediated p-STAT3 downregulation was caused by an increase in SHP-1 activity. Together, these findings suggest that the effect of this agent on SHP-1 activation was independent of kinase activation. Therefore, SC-1 was used as a starting point from which to generate SHP-1-activating agents with low-micromolar potency.

3.2. Lead optimization

SC-1 was first conjugated with different substituents through various linkers at the terminal amino group, generating compounds **1–12**. These derivatives were analyzed by MTT to determine cell growth inhibition within the dose range of 0.1–15 μ M in PLC5 cell (Table 1). Among these derivatives, urea derivatives showed robust cell growth inhibition, while the sulfonylamide counterparts showed moderate potency even at 7.5 μ M, and amide and amino linkers showed little effect. This differential increase in potency suggests a unique mode of ligand recognition that prefers planar geometry. The 4- to 5-fold improvement in the cell growth inhibition of compound **2** over SC-1 indicates the importance of this planar geometry interaction in ligand binding. Our data also showed that the *meta* substituent of benzene was better than the *para* substituent at inhibiting cell growth. For example, the only difference between compound SC-1 and compound **6** is the *meta* and *para* position for the conjunction in the benzene, however, the cell growth inhibition of compound **6** was at least one order of magnitude greater than that of SC-1.

With the pyridinyl ring moiety of sorafenib, we further examined the effect of modifying the urea moiety on cell growth inhibition. Among the four different analogs of sorafenib examined, the

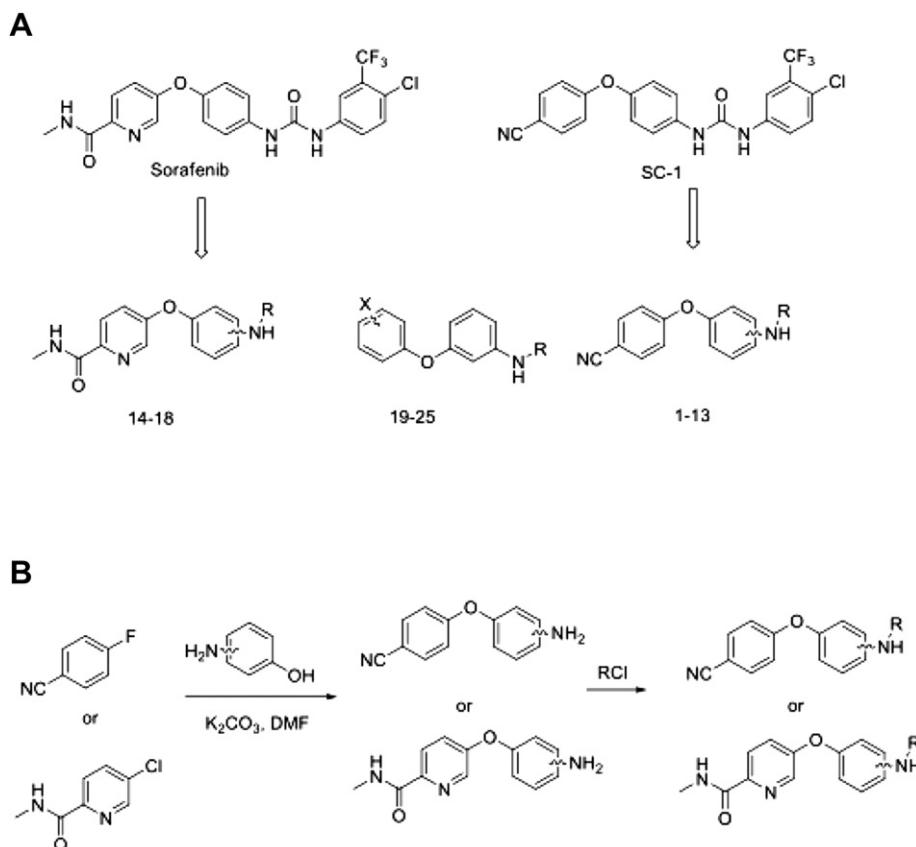


Fig. 1. (A) Representative structures of sorafenib and derivatives and (B) the general synthetic procedure for sorafenib derivatives.

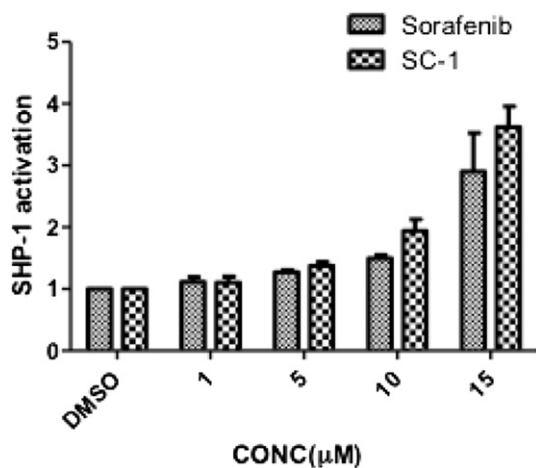


Fig. 2. Effects of sorafenib and SC-1 on SHP-1 activity. Dose effects of sorafenib and SC-1 on SHP-1 activation in PLC5 cells. Cells were treated with drugs at the indicated concentrations for 24 h. Columns, mean; bars, SD ($N = 3$).

sulfonylamide with phenyl trifluoromethane derivative (compound **14**) exhibited the highest potency, while the amide, amino methylene and phenyl sulfonyl derivative counterparts (**15–17**, respectively) showed no appreciable reduction in cell growth (Table 2). Next, we replaced the phenylcyano group of SC-1 with di-amino, nitro-amino and benzoimidazol-2-one to generate compounds **18–24**. As compared to these derivatives, compounds **18–20** bearing the nitro substituents showed more potent growth inhibition against PLC5 cells with IC_{50} values of 8.3, 3.9, and 1.2 μ M, respectively, whereas electron-donating substituted compounds such as **21**, and **22** revealed no appreciable cell growth inhibition (Table 3). These results indicate that a certain degree of electron withdrawing in the aromatic system is favorable for growth-inhibitory activity.

3.3. Effect of derivatives on downregulation of p-STAT3 through SHP-1 activation

Previously, we demonstrated that sorafenib and SC-1 repressed STAT3 phosphorylation through increasing SHP-1 activity. Here, we carried out three experiments to validate the mechanism by which the newly synthesized SC-1 derivatives mediate dephosphorylation of STAT3. First, to demonstrate the dephosphorylation ability of these derivatives, we assessed p-STAT3 inhibition by ELISA. As shown in Fig. 3, the derivatives which inhibited cell growth most effectively significantly reduced the level of p-STAT3, whereas the derivatives that did not inhibit cell growth did not inhibit p-STAT3. For example, compound **6** and compound **2** showed close correlation between reduction of p-STAT3 and cell growth.

Second, to understand the effect of the new derivatives on SHP-1, we further examined their induction of SHP-1 phosphatase activity. PLC5 cells were exposed to compounds **2**, **6**, and **16** at 10 μ M for 24 h and then cell lysates were collected for detection of SHP-1 activity. Compounds **2**, and **6** showed significantly increased SHP-1 activity in PLC5 cells, whereas compound **16** showed no appreciable change (Fig. 4A). Also, compound **6** enhanced SHP-1 activation in a dose dependent manner (Fig. 4B). These data imply that these compounds enhanced SHP-1 phosphatase activity and further reduced the p-STAT3 level.

Third, we validated the downstream signals of compounds **6** and **16** in PLC5 cells. As shown, at concentrations of 5 and 10 μ M compound **6** was effective in inhibiting p-STAT3 and subsequently repressing the expression of its target genes, such as Mcl-1, cyclin

Table 1

Chemical structure of compounds **1–12** and IC_{50} of growth inhibition in PLC5 cells. Cells were treated with drugs for 24 h and IC_{50} were measured in MTT assay.

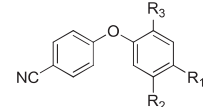
|  | | | | | |
|---|----------------|----------------|----------------|------------------------------------|--|
| Cpd | R ₁ | R ₂ | R ₃ | IC_{50} (μ M) in PLC5 cells | |
| SC-1 | | | | 7.5 | |
| 1 | | H | H | 12.3 | |
| 2 | | H | H | 2.1 | |
| 3 | | H | H | 10.5 | |
| 4 | | H | H | >15 | |
| 5 | | H | H | >15 | |
| 6 | H | | H | 0.5 | |
| 7 | H | | H | 2.2 | |
| 8 | H | | H | >15 | |
| 9 | H | | H | 3.3 | |
| 10 | H | | H | >15 | |
| 11 | H | | H | >15 | |
| 12 | H | | Me | 4.5 | |

Table 2

Chemical structure of compounds **13–17** and IC_{50} of growth inhibition in PLC5 cells. Cells were treated with drugs for 24 h and IC_{50} were measured in MTT assay.

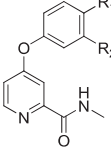
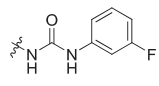
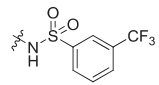
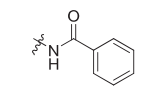
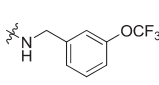
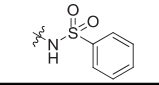
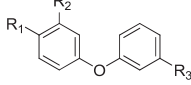
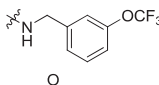
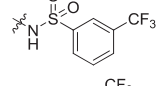
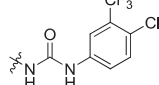
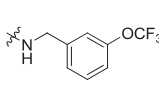
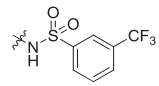
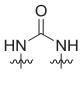
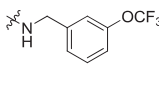
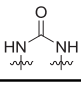
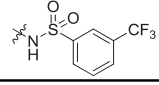
| Cpd | R ₁ | R ₂ | IC_{50} (μ M) in PLC5 cells |
|---|----------------|---|------------------------------------|
|  | | | |
| 13 | H |  | >15 |
| 14 | H |  | 8.4 |
| 15 | H |  | >15 |
| 16 | H |  | >15 |
| 17 | H |  | >15 |

Table 3

Chemical structure of compounds **18–24** and IC_{50} of growth inhibition in PLC5 cells. Cells were treated with drugs for 24 h and IC_{50} were measured in MTT assay.

| Cpd | R ₁ | R ₂ | R ₃ | IC_{50} (μ M) in PLC5 cells |
|---|---|-----------------|---|------------------------------------|
|  | | | | |
| 18 | NO ₂ | NH ₂ |  | 8.3 |
| 19 | NO ₂ | NH ₂ |  | 3.9 |
| 20 | NO ₂ | NH ₂ |  | 1.2 |
| 21 | NH ₂ | NH ₂ |  | >15 |
| 22 | NH ₂ | NH ₂ |  | >15 |
| 23 |  | |  | 10.2 |
| 24 |  | |  | 11.5 |

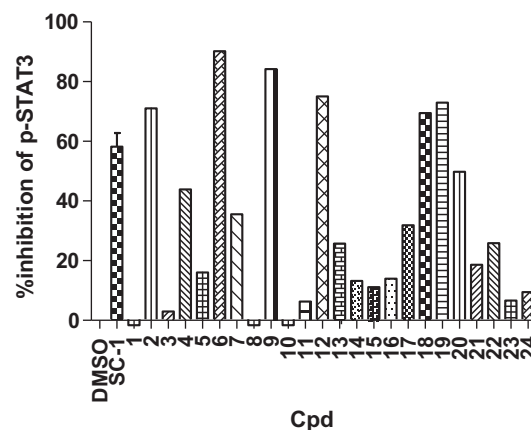


Fig. 3. ELISA analysis of the inhibitory effects of compounds **1–24** versus DMSO, each at 10 μ M, on the IL-6 stimulated p-STAT3 in PLC5 cells after 24 h of treatment. Columns, mean; bars, SD ($N = 3$).

D1 and survivin. On the other hand, compound **16** had no effect on the reduction of p-STAT3 and further signaling cascades (Fig. 5). Moreover, PLC5 treated with compound **6** showed significant cleavage of PARP-1 after a 24 h exposure suggesting apoptotic cell death. We also examined SOCS proteins, the negative regulator of Jak2/STAT pathway, upon drug treatment. Our data showed that compounds **6** and **16** did not affect the protein levels of SOCS-1 or SOCS-3.

Taken together, these data confirmed that the SC-1 derivatives mediated the repression of p-STAT3 through the same mechanism of action as SC-1, i.e., through SHP-1 activation. However, the exact mechanism of SC-1 derivative-induced SHP-1 activation remains unclear and will be further investigated in our lab.

3.4. Effects of compound **2** in a PLC5 xenograft nude mouse model

To assay whether the biological effect of compound **2**, is potentially clinically relevant, we tested the *in vivo* effect of compound **2** on tumor growth in PLC5 bearing xenograft mice. PLC5-bearing mice were treated with vehicle (Cremophor EL/95% ethanol (50:50; Sigma)) or compound **2** perorally (p.o.) at 10 mg/kg/day for three weeks. As shown in Fig. 6A, compound **2** strongly inhibited the growth of PLC5 xenograft tumors. To further confirm the molecular mechanism of compound **2** and its anti-cancer effect in xenograft nude mice model, tumor extracts from vehicle and compound **2**-treated mice were assayed for p-STAT3 by western blot. p-STAT3 was repressed in compound **2**-treated tumor (Fig. 6B, right panel). We further examined SHP-1 activity in compound **2**-treated PLC5 xenograft. Compound **2**-treated tumors showed significant upregulation of SHP-1 activity *in vivo*.

4. Discussion

On the basis of previous mechanistic data showing that the effect of sorafenib on SHP-1 activation was independent of kinase inhibition, in this study we structurally modified sorafenib to develop a novel class of SHP-1-activating agents. Our hypothesis that the SHP-1 activation and p-STAT3 repression seen in sorafenib could be structurally dissociated was borne out by the compound SC-1, which, devoid of kinase activity, exhibited the same SHP-1-activating activity as sorafenib. Presumably, the phenylcyano component of SC-1, which has no hydrogen donor ability, reduces its interaction with kinase in the ATP binding domain. Subsequent modification of SC-1 by adding various linkers, including urea,

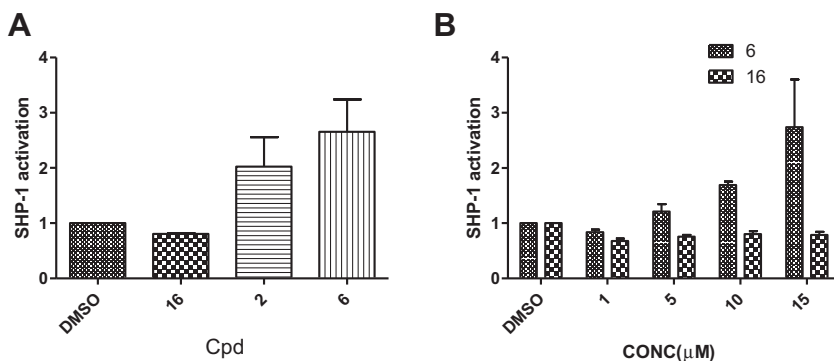


Fig. 4. Effects of new derivatives on SHP-1. (A) SHP-1 activity assay with compounds **2**, **6**, and **16** at 10 μM. Columns, mean; bars, SD ($n = 3$)/ $P < 0.05$. (B) Dose effects of compound **6** or **16** on SHP-1 activation in PLC5 cells. Cells were treated with drugs at the indicated concentrations for 24 h. Columns, mean; bars, SD ($N = 3$).

methylene urea, sulfonamide, amide, and amino groups resulted in different geometries and hydrogen bond proton donor ability. Among them, urea, methylene urea showed a multifold increase in SHP-1 activity in comparison with sulfonamide, and amide groups. This increase suggests that planar geometry favors SHP-1 activation. Moreover, a comparison of the substitution position of benzene in SC-1 and compound **6** showed that *meta* substitution greatly enhanced SHP-1 activation. Further modifications of the N-methylpicolinamide moiety revealed that electron withdrawing groups activate SHP-1 more strongly than electron-donating groups. For example, nitro and benzoimidazol-2-one resulted in significantly stronger SHP-1 activation than amino groups. It is also noteworthy that the SHP-1 activation by compound **6** was linked to biological and pharmacological activity in vivo and in vitro, i.e., compound **6** activates SHP-1 phosphatase and removes the phosphor group of STAT3 in PLC5 cells. This action impedes STAT3 transcription activation and subsequently represses proliferation and survival genes such as Mcl-1, cyclin D1 and survivin in PLC5 cells. Equally important, compound **2** was shown to mediate tumor growth inhibition in a nude mouse xenograft model. Thus, from

a mechanistic perspective, compound **2** provides a useful pharmacological tool to study SHP-1 activation.

5. Conclusion

SC-1 derivatives represent the first series of small-molecule agents that exhibit potent enhancement of SHP-1 activation. These agents may have clinical relevance in light of the pivotal role of STAT3 in promoting tumorigenesis and drug resistance. In HCC, overexpression of STAT3 confers resistance to chemotherapy drugs and represents an oncoprotein drug target. The findings presented here point to the potential use of SHP-1-activating agents in the treatment of hepatocellular carcinoma.

6. Experimental section

6.1. Materials

All commercially available starting materials were purchased from Sigma–Aldrich, or Acros and were used without further purification. Proton nuclear magnetic resonance (^1H NMR) spectra were recorded on Bruker DPX400 (400 MHz) instruments. Chemical shifts are reported as ppm. Reaction progress was determined by thin layer chromatography (TLC) analysis on silica gel 60 F254 plates (Merck). Chromatographic purification was carried out on silica gel 60 (0.063–0.200 mm or 0.040–0.063 mm, Merck), basic silica gel. High resolution mass spectra were recorded on a Finnigan MAT 95S mass spectrometer. Sorafenib (Nexavar) was kindly provided by Bayer Pharmaceuticals (West Haven, CT). Sodium vanadate and SHP-1 inhibitor were purchased from Cayman Chemical (Ann Arbor, MI). Antibodies for immunoblotting such as Cyclin D1, and PARP were purchased from Santa Cruz Biotechnology (San Diego, CA). Other antibodies such as anti-SOCS-3, Mcl-1, survivin, phospho-STAT3 (Tyr705), and STAT3 were from Cell Signaling (Danvers, MA).

6.2. Chemical synthesis

6.2.1. General procedures for the synthesis of compounds **1–13**

To a 50 mL THF solution of triphosgen (0.30 g, 1.0 mmol), aniline (1.1 mmol) and 2 equivalent of triethyl amine were added. The mixture was heated to 50 °C for 30 min. After the temperature was back to room temperature, aminophenoxyl-benzonitrile in the 10 mL THF solution was added to the mixture and heated to 50 °C for another 30 min. The mixture was evaporated, diluted with water and extracted with EtOAc. The extract was washed with brine, dried over anhydrous magnesium sulfate, and concentrated under reduced pressure to give desired compound **1–13**.

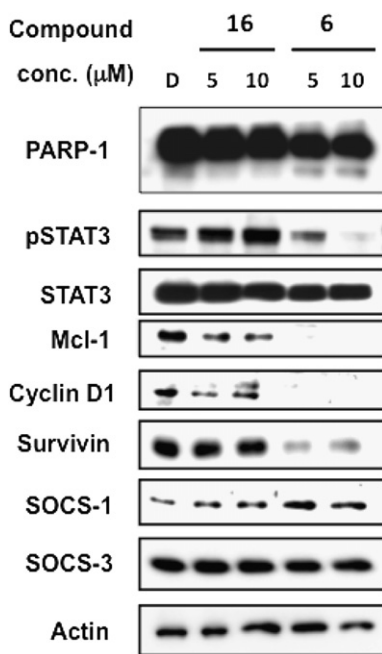


Fig. 5. Western blot analysis of the effect of compounds **6** and **16** each at 5 μM and 10 μM on the phosphorylation of STAT3, STAT3, Mcl-1, cyclin D1, survivin, SOCS-1, SOCS-3, and PARP-1 in PLC5 cells with serum-free medium after treatment for 24 h.

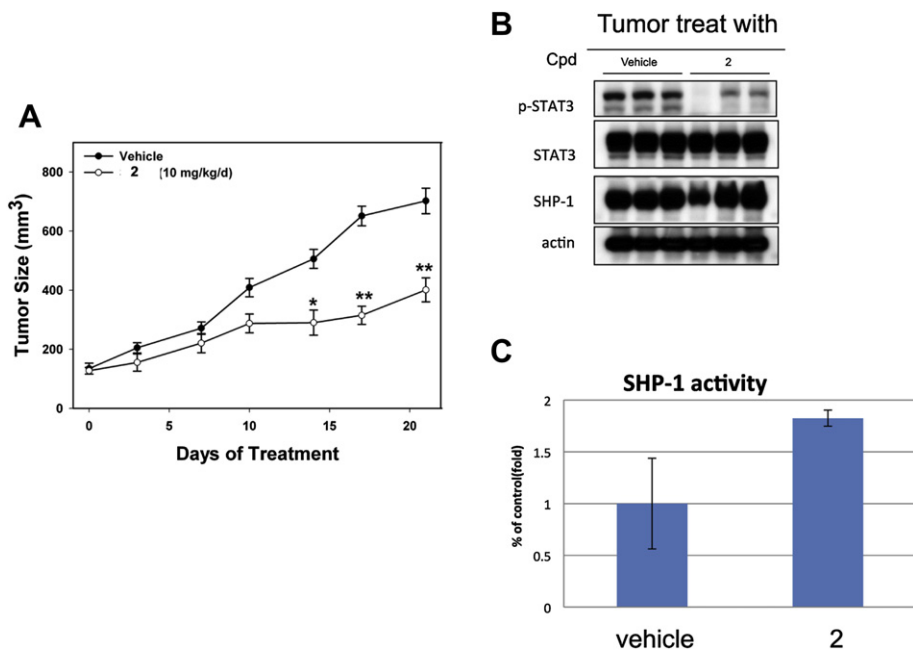


Fig. 6. In vivo effect of compound **2** on PLC5 xenograft nude mice. (A) Compound **2** shows a significant antitumor effect on PLC5 tumors. Top panel, points, mean ($n = 6$); bars, SE. Lower right panel, (B) Western blot analysis of p-STAT3, STAT3, and SHP-1 in PLC5 tumors. (C) SHP-1 activity in PLC5 tumors.

6.2.1.1. 1-(4-(4-Cyanophenoxy)phenyl)-3-(3,4-dimethoxybenzyl)urea (**1**). ¹H NMR (400 MHz, CDCl₃): δ 7.56 (d, $J = 6.8$ Hz, 2H), 7.34 (d, $J = 8.8$ Hz, 2H), 6.98–6.94 (m, 4H), 6.88–6.75 (m, 4H), 6.56 (brs, 1H), 4.36 (s, 2H), 3.84 (s, 6H); HRMS calculated for C₂₃H₂₀N₃O₄ [M – H][–]: 402.1454. Found: 402.1462.

6.2.1.2. 1-(4-Chloro-3-(trifluoromethyl)phenyl)-3-(4-(4-cyanophenoxy)benzyl)urea (**2**). ¹H NMR (400 MHz, CDCl₃): δ 7.76 (s, 1H), 7.51–7.39 (m, 3H), 7.29 (dd, $J = 8.8$ Hz, 2.4 Hz, 1H), 7.13 (d, $J = 8.4$ Hz, 3H), 6.83 (dd, $J = 8.8$ Hz, 4.8 Hz, 4H), 5.93 (t, $J = 6.0$ Hz, 1H), 4.24 (d, $J = 6.0$ Hz, 2H); ¹³C NMR (100 MHz, MeOD): δ 163.2, 157.5, 155.3, 140.6, 137.9, 135.4, 132.9, 130.3, 129.1 (m), 125.6, 124.9, 123.8, 122.9, 122.7, 1215, 119.6, 119.0, 118.4 (m), 106.7, 43.9; HRMS calculated for C₂₂H₁₄N₃O₂F₃Cl [M – H][–]: 444.0727. Found: 444.0732.

6.2.1.3. 1-(4-(4-Cyanophenoxy)benzyl)-3-(3,4-dimethoxybenzyl)urea (**3**). ¹H NMR (400 MHz, DMSO): δ 7.81 (d, $J = 9.2$ Hz, 2H), 7.33 (d, $J = 8.4$ Hz, 2H), 7.06 (dd, $J = 15.6$ Hz, 9.2 Hz, 4H), 6.86 (d, $J = 9.2$ Hz, 2H), 6.76 (dd, $J = 8.0$ Hz, 2.0 Hz, 1H), 6.45 (t, $J = 6.0$ Hz, 1H), 6.38 (t, $J = 6.0$ Hz, 1H), 4.23 (d, $J = 5.2$ Hz, 2H), 4.14 (d, $J = 5.2$ Hz, 2H), 3.69 (s, 6H); ¹³C NMR (100 MHz, DMSO-*d*₆): δ 161.4, 158.0, 152.9, 148.6, 147.6, 138.1, 134.6, 133.2, 128.9, 120.2, 119.0, 118.7, 117.7, 111.7, 111.1, 104.8, 55.5, 55.3, 42.8, 42.3; HRMS calculated for C₂₄H₂₄N₃O₄ [M + H]⁺: 418.1767. Found: 418.1773.

6.2.1.4. 1-(4-(4-Cyanophenoxy)benzyl)-3-(3-(trifluoromethoxy)benzyl)urea (**4**). ¹H NMR (400 MHz, CDCl₃): δ 7.49 (d, $J = 9.2$ Hz, 2H), 7.17 (t, $J = 8.0$ Hz, 1H), 7.10 (d, $J = 8.4$ Hz, 2H), 7.00–6.92 (m, 3H), 6.88 (d, $J = 9.2$ Hz, 2H), 6.84 (d, $J = 8.4$ Hz, 2H), 6.17–6.05 (m, 2H), 4.10 (m, 4H); ¹³C NMR (100 MHz, DMSO-*d*₆): δ 163.3, 160.8, 155.2, 150.7, 150.7, 144.4, 138.5, 135.4, 131.0, 130.1, 126.8, 125.7, 123.1, 121.4, 120.6, 10.5, 120.3, 119.6, 118.9, 118.1, 106.7, 44.1, 44.1; HRMS calculated for C₂₃H₁₉N₃O₃F₃ [M + H]⁺: 442.1379. Found: 442.1381.

6.2.1.5. (R)-1-(4-(4-Cyanophenoxy)phenyl)-3-(1-(naphthalen-1-yl)ethyl)urea (**5**). ¹H NMR (400 MHz, MeOD): δ 8.17 (d, $J = 8.0$ Hz, 1H), 7.87 (d, $J = 8.0$ Hz, 1H), 7.78 (d, $J = 8.0$ Hz, 1H), 7.65 (d, $J = 8.8$ Hz,

2H), 7.58 (d, $J = 7.2$ Hz, 1H), 7.53 (d, $J = 7.2$ Hz, 1H), 7.50–7.45 (m, 2H), 7.41 (d, $J = 8.8$ Hz, 2H), 6.99 (t, $J = 9.2$ Hz, 4H), 5.74 (d, $J = 6.8$ Hz, 1H), 1.63 (d, $J = 6.8$ Hz, 3H); HRMS calculated for C₂₆H₂₀N₃O₂ [M – H][–]: 406.1556. Found: 406.1563.

6.2.1.6. 1-(3-(4-Cyanophenoxy)phenyl)-3-(4-chloro-3-(trifluoromethyl)phenyl)urea (**6**). ¹H NMR (400 MHz, DMSO): δ 9.17 (s, 1H), 9.03 (s, 1H), 8.04 (d, $J = 2.4$ Hz, 1H), 7.83 (d, $J = 8.8$ Hz, 2H), 7.64–7.55 (m, 2H), 7.41–7.32 (m, 2H), 7.23 (d, $J = 7.2$ Hz, 1H), 7.11 (d, $J = 8.0$ Hz, 2H), 6.75 (dd, $J = 8.0$ Hz, 2.4 Hz, 1H); ¹³C NMR (100 MHz, DMSO-*d*₆): δ 161.0, 154.8, 152.3, 141.2, 139.1, 134.6, 132.0, 130.5, 127.3, 126.8, 126.5, 126.2, 124.1, 123.2, 122.5, 121.4, 118.7, 118.1, 116.9 (m), 115.1, 113.7, 110.0, 105.1; HRMS calculated for C₂₁H₁₂N₃O₂F₃Cl [M – H][–]: 430.0570. Found: 430.0576.

6.2.1.7. 4-(3-(3-(Trifluoromethyl)benzen-sulfonylamino)phenoxy)benzonitrile (**7**). ¹H NMR (400 MHz, CDCl₃): δ 8.00 (s, 1H), 7.96 (d, $J = 8.0$ Hz, 1H), 7.81 (d, $J = 8.0$ Hz, 1H), 7.65–7.54 (m, 3H), 7.26 (t, $J = 8.0$ Hz, 1H), 7.08 (s, 1H), 7.05–6.97 (m, 1H), 6.94–6.86 (m, 3H), 6.84 (t, $J = 2.0$ Hz, 1H), 6.81 (dd, $J = 8.4$ Hz, 2.0 Hz, 1H); HRMS calculated for C₂₀H₁₂N₂O₃F₃S [M – H][–]: 417.0521. Found: 417.0518.

6.2.1.8. 4-(3-(3-(Trifluoromethoxy)benzylamino)phenoxy)benzonitrile (**8**). ¹H NMR (400 MHz, CDCl₃): δ 7.61 (d, $J = 8.8$ Hz, 2H), 7.43 (t, $J = 8.0$ Hz, 1H), 7.33 (d, $J = 8.4$ Hz, 1H), 7.29–7.16 (m, 3H), 7.04 (d, $J = 8.8$ Hz, 2H), 6.55 (dd, $J = 8.0$ Hz, 2.4 Hz, 1H), 6.46 (dd, $J = 8.0$ Hz, 2.0 Hz, 1H), 6.34 (t, $J = 2.4$ Hz, 1H), 4.41 (s, 2H); ¹³C NMR (100 MHz, CDCl₃): δ 161.5, 155.9, 149.5 (m), 141.3, 133.9, 130.7, 130.0, 125.4, 124.2, 121.6, 119.7, 119.6, 119.1, 118.9, 117.9, 116.5, 109.8, 109.2, 105.5, 104.4, 47.4; HRMS calculated for C₂₁H₁₆N₂O₂F₃ [M + H]⁺: 385.1164. Found: 385.1157.

6.2.1.9. 1-(3-(4-Cyanophenoxy)phenyl)-3-(3-fluorophenyl)urea (**9**). ¹H NMR (400 MHz, MeOD): δ 7.66 (d, $J = 9.2$ Hz, 2H), 7.60 (s, 1H), 7.41–7.34 (m, 2H), 7.22 (q, $J = 8.0$ Hz, 1H), 7.18 (dd, $J = 8.0$ Hz, 2.0 Hz, 1H), 7.10–7.02 (m, 3H), 6.71 (dd, $J = 8.8$ Hz, 2.4 Hz, 2H); ¹³C NMR (100 MHz, MeOD): δ 165.6, 163.2, 162.9, 156.7, 154.6, 142.3,

142.2, 142.1, 135.3, 131.4, 131.1, 131.0, 119.6, 119.1, 116.5, 115.5, 115.3, 112.1, 110.1, 109.9, 107.2, 106.9, 106.7; HRMS calculated for $C_{20}H_{13}N_3O_2$ $[M - H]^-$: 346.0992. Found: 346.0999.

6.2.1.10. N-(3-(4-Cyanophenoxy)phenyl)benzamide (10). 1H NMR (400 MHz, $CDCl_3$): δ 8.82 (s, 1H), 7.75 (d, J = 7.6 Hz, 2H), 7.53 (s, 1H), 7.46–7.35 (m, 4H), 7.28 (t, J = 8.0 Hz, 2H), 7.22 (t, J = 8.0 Hz, 1H), 6.90 (d, J = 8.8 Hz, 2H), 6.72 (dd, J = 8.0 Hz, 2.0 Hz, 1H); HRMS calculated for $C_{20}H_{13}N_2O_2$ $[M - H]^-$: 313.0977. Found: 313.0971.

6.2.1.11. N-(3-(4-Cyanophenoxy)phenyl)benzenesulfonamide (11). 1H NMR (400 MHz, $CDCl_3$): δ 7.79 (d, J = 8.4 Hz, 2H), 7.53 (t, J = 4.4 Hz, 3H), 7.42 (t, J = 8.0 Hz, 2H), 7.20 (t, J = 8.0 Hz, 1H), 6.93 (dd, J = 8.0 Hz, 2.0 Hz, 1H), 6.86–6.83 (m, 3H), 6.73 (dd, J = 8.0 Hz, 2.0 Hz, 1H); HRMS calculated for $C_{19}H_{13}N_2O_3S$ $[M - H]^-$: 349.0647. Found: 349.0643.

6.2.1.12. 1-(4-Chloro-3-(trifluoromethyl)phenyl)-3-(3-(4-cyanophenoxy)-4-methylphenyl)urea (12). 1H NMR (400 MHz, MeOD): δ 7.87 (d, J = 2.8 Hz, 1H), 7.60 (d, J = 9.2 Hz, 2H), 7.54 (dd, J = 8.4 Hz, 2.4 Hz, 1H), 7.39 (d, J = 8.8 Hz, 1H), 7.25 (d, J = 2.4 Hz, 1H), 7.18 (d, J = 8.0 Hz, 1H), 7.12 (dd, J = 8.0 Hz, 2.4 Hz, 1H), 6.93 (d, J = 9.6 Hz, 2H), 2.02 (s, 3H); ^{13}C NMR (100 MHz, MeOD): δ 163.0, 154.5, 153.8, 139.9, 139.7, 135.4, 132.9, 129.7, 129.4, 129.1, 128.8, 126.2, 125.7, 125.5 (m), 124.1, 122.8, 120.1, 119.7, 118.6 (m), 118.0, 117.6, 117.5, 113.2, 113.1, 106.2, 15.5; HRMS calculated for $C_{22}H_{14}N_3O_2F_3Cl$ $[M - H]^-$: 444.0727. Found: 444.0725.

6.2.1.13. 1-(3-(2-(Methylcarbamoyl)pyridin-4-yloxy)phenyl)-3-(3-fluorophenyl)urea (13). 1H NMR (400 MHz, DMSO- d_6): δ 8.97 (d, J = 9.6 Hz, 2H), 8.77 (d, J = 4.8 Hz, 1H), 8.51 (d, J = 5.6 Hz, 1H), 7.50–7.35 (m, 4H), 7.28 (t, J = 8.4 Hz, 2H), 7.18 (d, J = 5.6 Hz, 1H), 7.09 (d, J = 8.4 Hz, 1H), 6.82 (d, J = 8.0 Hz, 1H), 6.77 (t, J = 8.4 Hz, 1H), 2.77 (d, J = 4.8 Hz, 3H); ^{13}C NMR (100 MHz, DMSO- d_6): δ 165.5, 163.9, 163.5, 161.2, 153.7, 152.5, 152.3, 150.6, 141.6, 141.4, 141.3, 130.8, 130.5, 130.4, 115.7, 114.51, 114.2, 110.4, 109.1, 108.6, 108.4, 105.3, 105.0, 26.1; HRMS calculated for $C_{20}H_{18}N_4O_3F$ $[M + H]^+$: 381.1363. Found: 381.1358.

6.2.2. General procedures for the synthesis of compounds 14–24

In a 25 mL two-necked round flask, aniline derivatives (1 mmol) and catalytic amount of pyridine were placed in anhydrous THF (10 mL) at room temperature. Acyl chloride or sulfonyl chloride compounds were added to the mixture and stirred for 2 h at room temperature. The solvent was removed under vacuum and the crude residue purified by chromatography on a silica gel column using EtOAc/hexane as eluent (1/10 to 1/2). This procedure afforded the expected coupling product as a white solid from 80% to 95% yield.

6.2.2.1. 4-(3-(3-(Trifluoromethoxy)benzylamino)phenoxy)-N-methylpyridine-2-carboxamide (14). 1H NMR (400 MHz, $CDCl_3$): δ 8.31 (d, J = 5.6 Hz, 1H), 7.98 (brs, 1H), 7.70 (d, J = 2.4 Hz, 1H), 7.34 (t, J = 8.0 Hz, 1H), 7.26 (d, J = 7.6 Hz, 1H), 7.18–7.14 (m, 2H), 7.10 (d, J = 8.0 Hz, 1H), 6.90 (dd, J = 5.6 Hz, 2.4 Hz, 1H), 6.47 (dd, J = 8.0 Hz, 2.0 Hz, 1H), 6.39 (dd, J = 7.6 Hz, 2.0 Hz, 1H), 6.28 (t, J = 2.0 Hz, 1H), 4.31 (s, 2H), 4.27 (s, 1H), 2.98 (d, J = 4.8 Hz, 3H); ^{13}C NMR (100 MHz, $CDCl_3$): δ 166.2, 164.6, 154.9, 152.1, 149.7, 149.6, 149.5, 149.5, 141.3, 130.8, 130.0, 125.5, 124.2, 121.6, 119.7, 119.7, 119.1, 116.5, 114.1, 110.4, 110.3, 109.6, 104.8, 47.6, 26.0; HRMS calculated for $C_{21}H_{19}N_3O_3F_3$ $[M + H]^+$: 418.1379. Found: 418.1385.

6.2.2.2. 4-(3-(3-(Trifluoromethyl)benzene-sulfonylamino)phenoxy)-N-methylpyridine-2-carboxamide (15). 1H NMR (400 MHz, $CDCl_3$): δ 8.36 (d, J = 5.6 Hz, 1H), 8.20–8.08 (m, 2H), 7.93 (d, J = 8 Hz, 1H), 7.77 (d, J = 8 Hz, 1H), 7.60 (t, J = 8 Hz, 1H), 7.54 (d, J = 2.4 Hz, 1H),

7.25 (t, J = 8.4 Hz, 1H), 6.98–6.94 (m, 2H), 6.91 (dd, J = 5.6 Hz, 2.4 Hz, 1H), 6.82 (dd, J = 8.0 Hz, 2.0 Hz, 1H), 3.00 (d, J = 5.2 Hz, 3H); HRMS calculated for $C_{20}H_{17}N_3O_4F_3S$ $[M + H]^+$: 452.0892. Found: 452.0891.

6.2.2.3. 4-(3-(Benzene-carbonylamino)phenoxy)-N-methylpyridine-2-carboxamide (16). 1H NMR (400 MHz, $CDCl_3$): δ 8.37 (d, J = 5.2 Hz, 1H), 8.05 (s, 1H), 8.00 (brs, 1H), 7.84 (d, J = 8.0 Hz, 1H), 7.83 (s, 1H), 7.68 (d, J = 2.4 Hz, 1H), 7.62 (t, J = 2.0 Hz, 1H), 7.34–7.60 (m, 5H), 6.99 (dd, J = 5.2 Hz, 2.4 Hz, 1H), 6.86 (dt, J = 7.2 Hz, 2.0 Hz, 1H), 2.98 (d, J = 4.8 Hz, 3H); ^{13}C NMR (100 MHz, $CDCl_3$): δ 166.0, 165.7, 164.6, 154.2, 152.1, 149.7, 139.8, 134.5, 132.0, 130.6, 128.8, 127.0, 117.0, 116.6, 114.4, 112.7, 110.3, 26.1; HRMS calculated for $C_{20}H_{18}N_3O_3$ $[M + H]^+$: 348.1348. Found: 348.1345.

6.2.2.4. 4-(3-(Benzene-sulfonylamino)phenoxy)-N-methylpyridine-2-carboxamide (17). 1H NMR (400 MHz, MeOD): δ 8.43 (d, J = 5.6 Hz, 1H), 7.76 (d, J = 8.0 Hz, 2H), 7.60–7.54 (m, 1H), 7.50 (t, J = 8.0 Hz, 2H), 7.46 (d, J = 2.4 Hz, 1H), 7.31 (t, J = 8.0 Hz, 1H), 6.99 (dd, J = 8.0 Hz, 2.0 Hz, 1H), 6.91 (dd, J = 5.6 Hz, 2.4 Hz, 1H), 6.88 (t, J = 2.0 Hz, 1H), 6.83 (dd, J = 8.0 Hz, 2.0 Hz, 1H), 2.94 (s, 3H); HRMS calculated for $C_{19}H_{18}N_3O_4S$ $[M + H]^+$: 384.1018. Found: 384.1013.

6.2.2.5. N-(3-(Trifluoromethoxy)benzyl)-3-(3-amino-4-nitrophenoxy)benzenamine (18). 1H NMR (400 MHz, $CDCl_3$): δ 8.05 (d, J = 9.2 Hz, 1H), 7.34 (t, J = 8.0 Hz, 1H), 7.30–7.20 (m, 2H), 7.19–7.13 (m, 2H), 7.11 (d, J = 8.0 Hz, 1H), 6.47 (dd, J = 8.0 Hz, 2.0 Hz, 1H), 6.40 (dd, J = 8.0 Hz, 2.0 Hz, 1H), 6.32–6.26 (m, 2H), 6.12 (d, J = 2.8 Hz, 1H), 6.06 (brs, 2H), 4.33 (d, J = 5.2 Hz, 2H), 4.27 (d, J = 5.2 Hz, 1H); HRMS calculated for $C_{20}H_{17}N_3O_4F_3$ $[M + H]^+$: 420.1171. Found: 420.1165.

6.2.2.6. N-(3-(Trifluoromethyl)benzene-sulfonyl)-3-(3-amino-4-nitrophenoxy)benzenamine (19). 1H NMR (400 MHz, $CDCl_3$): δ 8.06 (d, J = 9.6 Hz, 1H), 8.00 (s, 1H), 7.96 (d, J = 8.0 Hz, 1H), 7.81 (d, J = 8.0 Hz, 1H), 7.61 (t, J = 8.0 Hz, 1H), 7.27 (t, J = 8.0 Hz, 1H), 6.91–6.80 (m, 3H), 6.19 (dd, J = 9.6 Hz, 2.4 Hz, 1H), 6.14 (d, J = 2.4 Hz, 1H), 6.10 (brs, 2H); ^{13}C NMR (100 MHz, $CDCl_3$): δ 163.1, 155.5, 146.7, 140.0, 137.6, 132.0, 131.6, 130.9, 130.3, 130.0, 129.9 (m), 128.8, 128.0, 124.4, 124.3, 124.2, 124.2, 124.0, 121.6, 117.8, 117.6, 113.6, 107.6, 104.3; HRMS calculated for $C_{19}H_{13}N_3O_5F_3S$ $[M - H]^-$: 452.0528. Found: 452.0529.

6.2.2.7. 1-(3-(3-Amino-4-nitrophenoxy)phenyl)-3-(4-chloro-3-(trifluoromethyl)phenyl) urea (20). 1H NMR (400 MHz, DMSO): δ 9.19 (s, 1H), 9.05 (s, 1H), 8.06 (d, J = 1.6 Hz, 1H), 8.00 (d, J = 9.6 Hz, 1H), 7.67–7.55 (m, 2H), 7.47 (s, 1H), 7.42–7.32 (m, 2H), 7.27 (d, J = 8.4 Hz, 1H), 6.78 (q, J = 8.0 Hz, 1H), 6.40 (d, J = 2.8 Hz, 1H), 6.29 (dd, J = 9.6 Hz, 2.4 Hz, 1H); HRMS calculated for $C_{20}H_{13}N_4OClF_3$ $[M - H]^-$: 465.0577. Found: 465.0584.

6.2.2.8. 4-(3-(3-(Trifluoromethoxy)benzylamino)phenoxy)benzene-1,2-diamine (21). 1H NMR (400 MHz, $CDCl_3$): δ 7.33 (t, J = 8.0 Hz, 1H), 7.27–7.22 (m, 1H), 7.18 (s, 1H), 7.10 (d, J = 8.0 Hz, 1H), 7.04 (t, J = 8.0 Hz, 1H), 6.62 (d, J = 8.4 Hz, 1H), 6.39 (d, J = 2.4 Hz, 1H), 6.36 (dd, J = 8.4 Hz, 2.4 Hz, 1H), 6.31–6.24 (m, 2H), 6.19 (t, J = 2.4 Hz, 1H), 4.28 (d, J = 5.6 Hz, 2H), 4.08 (t, J = 5.6 Hz, 1H), 3.44 (brs, 2H), 3.17 (brs, 2H); ^{13}C NMR (100 MHz, MeOD): δ 161.2, 151.4, 151.1, 150.7, 150.7, 144.5, 137.8, 131.3, 130.9, 130.7, 126.9, 125.7, 123.1, 120.5, 120.1, 118.4, 111.2, 109.2, 108.1, 107.1, 103.1, 47.9; HRMS calculated for $C_{20}H_{19}N_3O_2F_3$ $[M + H]^+$: 390.1429. Found: 390.1421.

6.2.2.9. 4-(3-(3-(Trifluoromethoxy)benzene-sulfonylamino)phenoxy)benzene-1,2-diamine (22). 1H NMR (400 MHz, $CDCl_3$): δ 7.96 (s, 1H), 7.88 (d, J = 8.0 Hz, 1H), 7.78 (d, J = 8.0 Hz, 1H), 7.56

(t, $J = 8.0$ Hz, 1H), 7.12 (t, $J = 8.0$ Hz, 1H), 6.70 (td, $J = 8.0$ Hz, 2.0 Hz, 2H), 6.61 (d, $J = 8.0$ Hz, 1H), 6.55 (t, $J = 2.0$ Hz, 1H), 6.32 (d, $J = 2.8$ Hz, 1H), 6.25 (dd, $J = 8.0$ Hz, 2.4 Hz, 1H), 3.84 (brs, 2H), 3.28 (brs, 2H); HRMS calculated for $C_{19}H_{17}N_3O_3F_3S$ $[M + H]^+$: 424.0943. Found: 424.0936.

6.2.2.10. 5-(3-((3-(Trifluoromethoxy)benzyl)amino)phenoxy)-1H-benzodimidazol-2(3H)-one (**23**). 1H NMR (400 MHz, MeOD): δ 7.33 (t, $J = 8.0$ Hz, 1H), 7.26 (d, $J = 7.6$ Hz, 1H), 7.16 (s, 1H), 7.08 (d, $J = 8.0$ Hz, 1H), 7.01–6.97 (m, 1H), 6.93 (d, $J = 8.4$ Hz, 1H), 6.66–6.60 (m, 2H), 6.31 (dd, $J = 8.0$ Hz, 2.4 Hz, 1H), 6.18 (dd, $J = 8.0$ Hz, 2.4 Hz, 1H), 6.09 (d, $J = 2.0$ Hz, 1H), 4.27 (s, 2H); HRMS calculated for $C_{21}H_{17}N_3O_3F_3$ $[M + H]^+$: 416.1222. Found: 416.1221.

6.2.2.11. N-(3-((2-Oxo-2,3-dihydro-1H-benzodimidazol-5-yl)oxy)phenyl)-3-(trifluoromethyl)benzenesulfonamide (**24**). 1H NMR (400 MHz, $CDCl_3$): δ 9.65 (brs, 2H), 7.99 (s, 1H), 7.91 (d, $J = 8.0$ Hz, 1H), 7.73 (d, $J = 8.0$ Hz, 1H), 7.53 (t, $J = 8.0$ Hz, 1H), 7.10 (t, $J = 8.0$ Hz, 1H), 6.85 (d, $J = 8.0$ Hz, 1H), 6.79 (d, $J = 8.0$ Hz, 1H), 6.66 (dd, $J = 8.0$ Hz, 2.0 Hz, 1H), 6.62–6.53 (m, 2H), 6.49 (s, 1H); HRMS calculated for $C_{20}H_{13}N_3O_4F_3S$ $[M - H]^-$: 448.0579. Found: 448.0588.

6.3. Biological assays

6.3.1. Cell culture

PLC5 cells were maintained in DMEM supplemented with 10% FBS, 100 units/mL penicillin G, 100 μ g/mL streptomycin sulfate and 25 μ g/mL amphotericin B in a 37 °C humidified incubator in an atmosphere of 5% CO_2 in air.

6.3.2. Cell viability analysis

The effect of individual test agents on cell viability was assessed by using the 3-(4,5-dimethylthiazol-2-yl)-2,5-diphenyltetrazolium bromide (MTT) assay in 6 replicates. Cells were seeded and incubated in 96-well, flat-bottomed plates for 24 h and were exposed to various concentrations of test agents dissolved in DMSO (final concentration, 0.1%) in DMEM. Controls received DMSO vehicle at a concentration equal to that in drug-treated cells. The medium was removed, replaced by 200 μ L of 0.5 mg/mL MTT in 10% fetal bovine serum-containing DMEM, and cells were incubated in the carbon dioxide incubator at 37 °C for 2 h. Supernatants were removed from the wells and the reduced MTT dye was solubilized in 200 μ L/well DMSO. Absorbance at 570 nm was determined on a plate reader.

6.3.3. Western blot

PLC5 cells were treated with compounds **6** and **16** at 5 and 10 μ M for 24 h. Cell lysates were analyzed by western blot.

6.3.4. Phospho-STAT3 ELISA assay

PLC5 cells were seeded in 6-well plates and pre-stimulated with IL-6 at the dose of 25 ng/mL for 30 min and then treated with 10 μ M sorafenib derivatives for 24 h. The STAT3 ELISA kit was purchased from Cell Signaling (Danvers, MA).

6.3.5. Phosphatase and kinase activity

The RediPlate 96 EnzChek_Tyrosine Phosphatase Assay Kit (R-22067) was used for SHP-1 activity assay (Molecular Probes, Carlsbad, CA).

6.3.6. Xenograft tumor growth

Male NCr athymic nude mice (5–7 weeks of age) were obtained from the National Laboratory Animal Center (Taipei, Taiwan). All experimental procedures using these mice were performed in accordance with protocols approved by National Taiwan University. When PLC5 tumors reached 100 mm³, mice received compound **2** (10 mg/kg) p.o. once daily. Controls received vehicle.

Acknowledgments

We thank the National Science Council, Taiwan (NSC98-2320-B-010-005-My3 and NSC-100-2325-B-010-007) and National Yang Ming University, Taiwan for financial support. C.W.S. also thanks the National Research Institute of Chinese Medicine for NMR support.

Appendix A. Supplementary material

Supplementary data related to this article can be found online at <http://dx.doi.org/10.1016/j.ejmech.2012.07.023>.

References

- [1] Y. Liu, C. Li, J. Lin, *Anticancer Agents Med. Chem.* 10 (2010) 512–519.
- [2] H. Wang, F. Lafdil, X. Kong, B. Gao, *Int. J. Biol. Sci.* 7 (2011) 536–550.
- [3] A. Kumanovics, S.L. Perkins, H. Gilbert, M.H. Cessna, N.H. Augustine, H.R. Hill, *J. Clin. Immunol.* 30 (2010) 886–893.
- [4] S. Dong, S.J. Chen, D.J. Tweardy, *Leuk. Lymphoma* 44 (2003) 2023–2029.
- [5] Q. Lin, R. Lai, L.R. Chirieac, C. Li, V.A. Thomazy, I. Grammatikakis, G.Z. Rassidakis, W. Zhang, Y. Fujio, K. Kunisada, S.R. Hamilton, H.M. Amin, *Am. J. Pathol.* 167 (2005) 969–980.
- [6] J.F. Bromberg, M.H. Wrzeszczynska, G. Devgan, Y. Zhao, R.G. Pestell, C. Albanese, J.E. Darnell Jr., *Cell* 98 (1999) 295–303.
- [7] L. Song, B. Rawal, J.A. Nemeth, E.B. Haura, *Mol. Cancer Ther.* 10 (2011) 481–494.
- [8] K.F. Chen, W.T. Tai, T.H. Liu, H.P. Huang, Y.C. Lin, C.W. Shiau, P.K. Li, P.J. Chen, A.L. Cheng, *Clin. Cancer Res.* 16 (2010) 5189–5199.
- [9] B.B. Aggarwal, A.B. Kunnumakkara, K.B. Harikumar, S.R. Gupta, S.T. Tharakan, C. Koca, S. Dey, B. Sung, *Ann. N. Y. Acad. Sci.* 1171 (2009) 59–76.
- [10] A. Liu, Y. Liu, P.K. Li, C. Li, J. Lin, *Anticancer Res.* 31 (2011) 2029–2035.
- [11] L. Liu, S. Nam, Y. Tian, F. Yang, J. Wu, Y. Wang, A. Scuto, P. Polychronopoulos, P. Magiatis, L. Skaltsounis, R. Jove, *Cancer Res.* 71 (2011) 3972–3979.
- [12] K.F. Chen, W.T. Tai, J.W. Huang, C.Y. Hsu, W.L. Chen, A.L. Cheng, P.J. Chen, C.W. Shiau, *Eur. J. Med. Chem.* 46 (2011) 2845–2851.
- [13] W.T. Tai, A.L. Cheng, C.W. Shiau, H.P. Huang, J.W. Huang, P.J. Chen, K.F. Chen, *J. Hepatol.* 55 (2011) 1041–1048.
- [14] R. Bhattacharya, J. Kwon, E. Wang, P. Mukherjee, D. Mukhopadhyay, *J. Mol. Signal.* 3 (2008) 8.
- [15] Z. Yu, L. Su, O. Hoglinger, M.L. Jaramillo, D. Banville, S.H. Shen, *J. Biol. Chem.* 273 (1998) 3687–3694.
- [16] H. Keilhack, T. Tenev, E. Nyakatura, J. Godovac-Zimmermann, L. Nielsen, K. Seedorf, F.D. Bohmer, *J. Biol. Chem.* 273 (1998) 24839–24846.
- [17] M. Thangaraju, K. Sharma, B. Leber, D.W. Andrews, S.H. Shen, C.B. Srikant, *J. Biol. Chem.* 274 (1999) 29549–29557.
- [18] H. Tassidi, Z. Culig, A.G. Wingren, P. Harkonen, *Prostate* 70 (2010) 1491–1500.